Numerical Calculation of Thermal Radiation View Factors

Kanokwan Buaprommart, Sergey Martynov, and Haroun Mahgerefteh
Department of Chemical Engineering, University College London, WC1E 7JE, London, U.K.

Abstract

A pipeline leakage is one of the most critical problems in the oil and gas industry, resulting in catastrophic accidents. Fires originating from pipeline rupture pose a serious hazard to steel structures and are the leading causes of severe injuries and fatalities. Consequently, an investigation of the potential risks of fires involving determining the distances in the case of fire-originating thermal radiation effects in deferent severity harm scenarios is crucial. The research project deals with the development of mathematical modelling of the transient fluid outflow model - linked to the fire model for simulating thermal radiation in the event of an accidental pipeline rupture. The fluid properties at the ruptured pipe, especially the fluid discharge flow rate, pressure and temperature, and the fluid's phase, are represented as initial conditions in the fire model. The source term model deals with the implementation of numerical methods, based on the Method of Characteristic (MOC) and Euler's predictor-corrector method, to solve pertinent conservation equations in the quasilinear hyperbolic form. The fluid variables obtained from this model are subsequently applied to the fire model, derived from the empirical flame characteristic model as well as the numerical method to estimate the radiation view factor to obtain: the relationship between the radiative intensity of the fire; the duration and the distance of the receiver object. The results obtained from these simulations are used in conjunction with the relevant published data.

Objectives

To improve the accuracy of the thermal radiation models for industrial fires by

(a) accounting for the flame and target geometries,

(b) developing a computational algorithm for calculating the radiation view factors between the flame and the target,

(c) predicting the transient phenomenon by coupling the jet fire model with the transient pipeline discharge flow model.

The discharge flow model

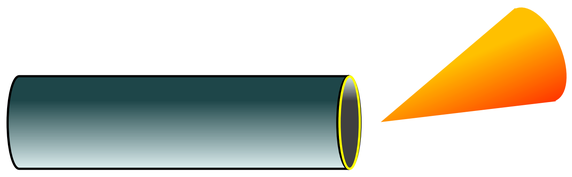

Figure 1. Discharge of igniting fuel.

To predict the history of decompression of pipeline the transient outflow model is adopted, based on the mass, momentum and energy conservation equations [1]:

$$\frac{\partial \rho}{\partial t} + \frac{\partial \rho u}{\partial x} = 0$$

$$\frac{\partial \rho u}{\partial t} + \frac{\partial \left(\rho u^2 + p\right)}{\partial x} = -\rho g_x - \frac{f_w \rho u^2}{D}$$

$$\frac{\partial \rho E}{\partial t} + \frac{\partial \left(\rho u E + u p\right)}{\partial x} = -\rho u g_x - \frac{f_w \rho u^3}{D} + q_w$$

where ρ, u, E, and p are respectively the fluid density, velocity, total specific energy and pressure, x is the spatial coordinate along the well in the direction of discharge flow. t is the time and D is the internal diameter of the pipe. Furthermore, g_x is the gravity force on the x axis. q_w is the heat flux at pipe wall and f_w is the Fanning friction factor.

The jet fire model

An average incident radiation flux received from the jet flame (object 2) by receiver (object 1) (Figure 2) is defined as [2]

$$q_r = \frac{Q}{A_1} = \tau E F_{1-2}$$

where τ, E, $F_{1\text{-}2}$, A_1 and $Q_{2\text{-}1}$ are atmospheric transmissivity, emissive power, radiation view factor exchange from object 1 to object 2, area of body 1 and total power transferred from the flame by thermal radiation, respectively.

A different set of axes and coordinates between the Johnson model [3] and the Davis & Bagster model [2] are implemented by translating the position of receiver and its surface normal.

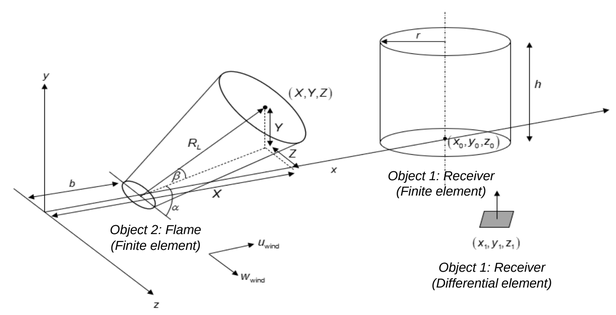

Figure 2. Configuration of the horizontal release flame shape model (object 2) where b, R_L, X, Y and Z are the flame lift-off, frustum length and X, Y and Z position of the end of the flame, respectively. α and β are the angle between the flame axis and release axis and the angle between x- axis and y-axis. u_{wind} and w_{wind} are wind speeds in the release direction and perpendicular to the release [3]. In addition, the receiver (object 1) is accounted for as the differential or finite element. x_1, y_1 and z_1 are the receiver position in x, y and z-coordinates. x_0, y_0 and z_0 are the centre of the tank in x, y and z-coordinates. h and r are the tank height and radius, respectively.

The view factor model

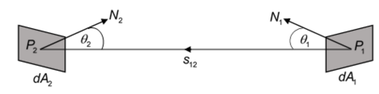

Figure 3. Configuration for radiative exchange between two differential elements. P_1 and P_2 are the positions of the receiver element and emitting surface. s_{12} is the vector from the position of the receiver element to a point on the boundary contour of the emitting surface. N_1 and N_2 are unit surface normal vectors of the receiver and emitter surface elements, respectively. θ_1 and θ_2 denote the angle between s_{12} and N_1 and N_2. dA_1 and dA_2 are an elemental area of receiver and emitter.

The view factor between differential and finite targets is obtained by [2]

$$F_{d1-2} = \int_{A_2} \frac{\cos\theta_1 \cos\theta_2}{\pi s^2} dA_2; \ \theta_1 \text{ and } \theta_2 \le 90°$$

Stokes' theorem can be used to convert to an equivalent contour integral. Linear superposition can be applied when the boundary curve is the same for all target orientations to obtain the maximum view factor [2].

$$\left(F_{d1-2}\right)_{\max} = \sqrt{F_x^2 + F_y^2 + F_z^2}$$

Where the *F* values are for targets oriented orthogonally.
A surface integral over finite area A_1 depends strongly upon the shape of A_1, which can be described by the parametric representation [4]

$$s_1(u,v) = (x_1, y_1, z_1)$$

where *u* and *v are coordinates of numerical integration, shown in Figure 8.* The view factor between the radiating flame and the receiver object is calculated as [4]

$$F_{1-2} = \frac{1}{A_1} \int_{u_1}^{u_2} \int_{v_1}^{v_2} F_{d1-2} \left\| \frac{\delta S_1}{\delta u} \times \frac{\delta S_1}{\delta v} \right\| dv du$$

where $F_{d1\text{-}2}$ is the view factor between a differential source and a finite target [2]

Results

The model validation

The model has been validated against the measurements and compared with predictions by the Johnson model [3].

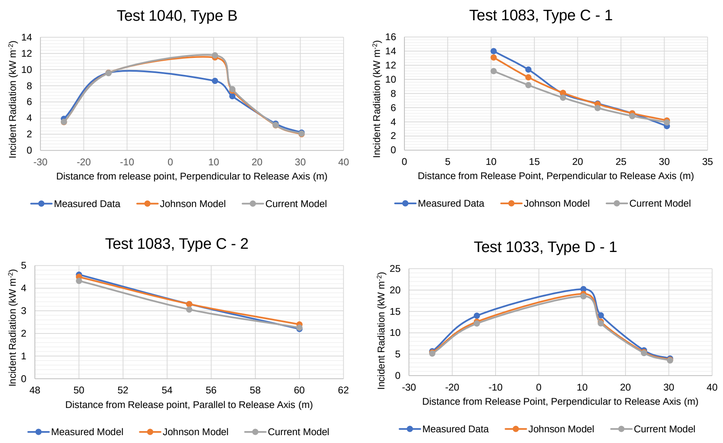

Figure 4. Comparison of measured radiation values with the predictions by the Johnson and the current study model.

Table 1. Experimental conditions of Test 1040, Type B, Test 1083, Type C-1, Test 1083, Type C-2, Test 1033, Type D-1 [3].

	Test 1040, Type B	Test 1083, Type C-1	Test 1083, Type C-2	Test 1033, Type D-1
Mass flow rate, kg s^{-1}	2.5	8.4	8.4	7.9
Stagnation pressure, barg	0.3	2.1	2.1	11.1
Stagnation temperature, K	277	267	267	279
Hole diameter, mm	152	152	152	75
Wind speed, m s^{-1}	1.7	0.3	0.3	3.9
Wind direction, degrees clockwise from North	247	326	326	271
Ambient temperature, K	279	281	281	282
Relative humidity, %	89	80	80	81
Receiver location (x, y, z), m	15, -0.5, -24.6 – 30.3	9, -2, 10.3 – 44.3	50 – 60, -2, 0.3	15, -2, 10.3 – 30.3
Jet release location (x, y, z), m	0, 0, 0	0, 0, 0	0, 0, 0	0, 0, 0
Gas velocity range	Subsonic	Sonic	Sonic	Sonic
Gas composition (Measured and Johnson)	94% Methane and other	94% Methane and other	94% Methane and other	94% Methane and other
Gas composition (Current model)	100% Methane	100% Methane	100% Methane	100% Methane

Parametric sensitivity study

Table 2. Main characteristics of the simulation

Parameters	Case 1	Case 2
Overall length	1000 m	1000 m
External diameter	168.28 mm	168.28 mm
Wall thickness	7.112 mm	7.112 mm
Failure mode	Puncture along pipeline length at 300 m	Full bore rupture at pipe end
Puncture diameter	50 mm	154.056 mm
Pipe orientation	0°	0°
Puncture orientation	40°	-
Composition	100% Methane	100% Methane
Fluid temperature	320 K	320 K
Fluid pressure	30, 50 and 100 bar	30 and 50 bar
Receiver object geometry and location in x-coordinate	Differential element (0-100 m)	Differential element (0-100 m)

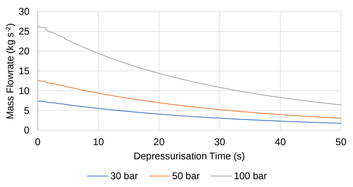

Figure 5. The calculated variation of the discharge flow rate versus time following rupture of the pipeline initially at the 30 bar, 50 bar and 100 bar pressure.

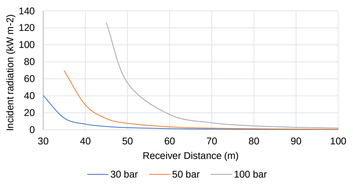

Figure 6. The incident heat flux from a jet fire predicted for Case 1 as a function of receiver distance at 0.1 s following the rupture of a pipeline initially at of 30 bar, 50 bar and 100 bar pressures.

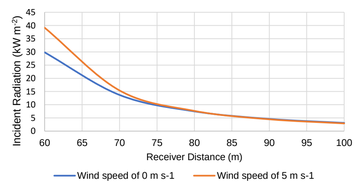

Figure 7. The incident heat flux as a function of receiver distance predicted for Case 2 following the full-bore rupture of a pipeline at 0.5 s for zero and 5 m s-1 wind speeds.

Key findings:

- The instant of rupture is signified by a high flow rate which reduces with time in a hyperbolic manner as the depressurises.
- As expected, the incident heat flux decreases with the distance from the centre of the horizontal jet.
- Higher wind speed in the receiver direction results in an increase of the incident heat flux.

Numerical convergence study

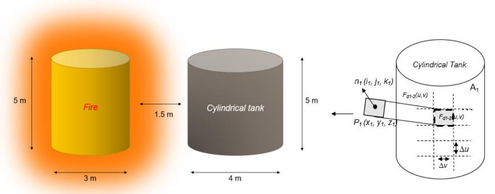

Figure 8. Schematic of the fire and tank in cylindrical shapes. A_1 is the area of the cylindrical tank. Δv and Δu are step size in v and u coordinates of numerical integration. $F_{d1\text{-}2i}$ is the view factor between each differential element (receiver element) and finite element (flame).

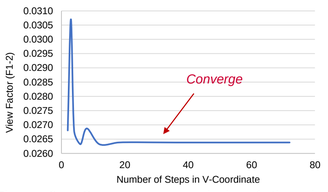

Figure 9a. Convergence analysis of the view factor between finite-finite targets, $F_{1\text{-}2}$, and number of step size in v-coordinate. Incremental change in u-coordinate, Δu, is fixed at 1 m. and incremental changes in v-coordinate, Δv, are varied from π/36 rad (5 deg) to π rad (180 deg).

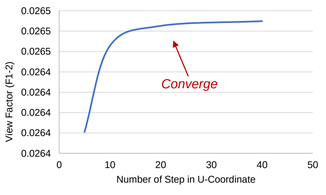

Figure 9b. Convergence analysis of the view factor between finite-finite targets, $F_{1\text{-}2}$, and number of step size in u-coordinate. Incremental change in v-coordinate, Δv, is fixed at π/9 rad (20 deg) and incremental changes in u-coordinate, Δu, are varied from 0.125 m to 1 m.

- The optimum number of step-size is attained at iterations of 18 and step size of π/9 rad (20 deg)
- The number of step-size yields convergence at approximate iterations of 20 and step size of 0.25 m

References

[1] H. Mahgerefteh, A. O. Oke, and Y. Rykov, "Efficient numerical solution for highly transient flows," *Chem. Eng. Sci.*, vol. 61, no. 15, pp. 5049–5056, 2006.

[2] B. C. Davis and D. F. Bagster, "The computation of view factors of fire models: 1. Differential targets," *Journal of Loss Prevention in the Process Industries*, vol. 2, no. 4, pp. 224–234, Jan. 1989

[3] A. D. Johnson, H. M. Brightwell, and A. J. Carsley, "A model for predicting the thermal radiation hazards from large-scale horizontally released natural gas jet fires," *Process Safety and Environmental Protection*, vol. 72, no. B3, pp. 157–166, 1994

[4] B. C. Davis and D. F. Bagster, "The computation of view factors of fire models: 2. Finite targets," *Journal of Loss Prevention in the Process Industries*, vol. 3, no. 3, pp. 327–329, Jul. 1990

UCL ENGINEERING
Change the world